Supplementary Information for

Density-dependent natural selection mediates harvest-induced trait changes

Alix Bouffet-Halle, Jacques Mériguet, David Carmignac, Simon Agostini, Alexis Millot, Samuel Perret, Eric Motard, Beatriz Decenciere, Eric Edeline*

* Corresponding author: eric.edeline@inrae.fr

This PDF file includes:

SI Appendix I: Supplementary Methods.
SI Appendix II: Natural selection on body size in medaka.
SI Appendix III: Supplementary Results:

- Table S1: Inference of number of age classes in pond medaka populations.
- Table S2: Structure and MCMC parameter estimates for models 4-6 and 8.
- Table S3: Effect of medaka fishing on medaka food in ponds.
- Table S4: Analysis of deviance.
- Fig. S1: Experimental design.
- Fig. S2: Random effects of breeding pairs on their progeny's somatic growth rate and maturation probability.

APPENDIX I. SUPPLEMENTARY METHODS

Origin of the experimental medaka populations

Our start medaka populations descended from 100 parents wild-caught in Kiyosu (Toyohashi, Aichi Prefecture, Japan) in June 2011. These 100 breeders were brought to the Centre de Recherche en Ecologie Expérimentale et Prédictive near Paris, France (CEREEP – ECOTRON Île-de-France, www.cereep.ens.fr), and maintained in groups of 20 individuals in five 20 L aquariums where they mated randomly. Eggs were collected from July to September 2011 and incubated in Petri dishes. Hatched larvae were randomly assigned to 12 circular outdoor ponds (3.57 m diameter, 1.2 m deep) at a density of about 160 larvae per pond which, we assumed, was sufficient to prevent founder effects.

Prior to medaka introduction, the 12 ponds were bottom-coated with a 5 cm layer of Loire River sand, filled with tap water and mildly enriched with a plant fertilizer. After a few weeks of algal development, tanks were seeded with a diverse community of zooplankton collected from surrounding water bodies. Medaka introduction was performed after ponds had reached a clear-water state indicating algal control by zooplankton. After introduction, two pairs of floating plastic brushes were placed in each tank to provide fish with a spawning substrate and shelter for larvae. Afterwards, ponds received only rain water and aerial deposits. Each pond was covered with a net to prevent avian predation, and outlets were secured with a stainless steel filter to prevent any fish or egg escapement.

Monitoring medaka food in ponds

In 2012, we measured the effect of medaka fishing in March on zooplankton and filamentous algae, which are primary food sources for medaka in ponds, during the following months. In each pond on 11 dates (April 11th and 27th, May 9th and 23rd, June 6th and 13th, July 4th and 18th, August 22nd and September 18th), zooplankton was sampled from twelve, 2 L water-column samples homogeneously spread across the pond. The resultant 24 L were filtered on a 50 µm filter and the retained zooplankton were fixed in 99% ethanol before subsequent enumeration of rotifers (*Asplanchna* sp. *vs*. other rotifers), Copepod *nauplii*, copepodite stages of calanoid and cyclopid Copepods, and Cladocerans using either a binocular microscope, the ZooScan (Gorsky *et al.* 2010) or the FlowCam (Sieracki *et al.* 1998). Percentage of pond surface covered by filamentous algae was visually estimated by multiple observers on 5 dates in 2012 (May 9th, September 18th and 24th, October 9th and 23rd) and 2 dates in 2013 (May 22nd and July 12th).

Feeding of F_1 progeny in the laboratory

In the low-food environment, medaka were fed once every second day with 2 mL of a solution containing *nauplii* of *Artemia salina* (INVE Aquaculture SEP-Art cysts) providing 8.2 ± 0.7 (mean ± SD) mg dry weight of *nauplii* (assuming a 40% dry weight yield from cysts from INVE technical sheets), alternated with dry food (Skretting Gemma Micro, see below). In the high-food environment, medaka were fed twice daily, once with *nauplii* and once with dry food. In the medium-food environment, medaka were fed once daily alternating *nauplii* and dry food.

Dry food doses (measured with volumetric spoons) and pellet sizes were adjusted during fish development to fit with the ontogenetic increase in energy needs and prey size. We computed theoretical daily needs in dry food mass per fish as $M(a)\times 0.30\left(M(a)/M_b\right)^{-0.25}$, where $M(a)$ is individual fish body mass at age *a* (as estimated from previous laboratory data on mass-age relationship in Renneville et al. 2020), M_b is individual fish body mass at birth, and the -0.25 exponent follows from the metabolic theory of ecology (Brown *et al.* 2004). To roughly follow these theoretical needs, medaka received daily 2, 3 and 7 mg of dry food from ages 0 to 40, 40 to 60, and 60 days-post-hatch (dph) onwards, respectively. Pellet size (µm) was 100% 150, 50% mixture of 150-300 and 100% 300 from ages 0 to 20, 20 to 40, and 40 dph onwards, respectively.

Statistical analyses

Fishery selection in ponds

We estimated the relationship between individual standard body length and probability to survive through the fishery using a Bernoulli GLMM with a logit link function:

$$\begin{aligned} & y_i \sim B(p_i) \\ & \ln\left(\frac{p_i}{1-pi}\right) = \alpha_0 + \alpha_{k[i]} + \left(\beta_0 + \beta_{k[i]}\right) Sdl_i \\ & \begin{pmatrix}\alpha_k \\ \beta_k\end{pmatrix} \sim N\left(\begin{pmatrix}0 \\ 0\end{pmatrix}, \begin{pmatrix}\sigma_\alpha & \rho\,\sigma_\alpha\sigma_\beta \\ \rho\,\sigma_\beta\sigma_\alpha & \sigma_\beta\end{pmatrix}\right) \end{aligned} \qquad (2),$$

where B is the Bernoulli distribution, subscripts i and k index individuals (*n* = 3970) and sampling events, respectively, to which individuals belong, and $\ln$ is the natural logarithm. There were n = 6 fished populations and n = 5 sampling years, yielding $k = 1,2 \ldots 30$ sampling events. Eq. 2 indicates that we modelled the intercept and slope of the survival-length relationship as normally-varying among sampling events k, including a correlation parameter ρ between intercept and slope. Parameter estimates α_0 and β_0 from Eq. 2 define a mean size-dependent survival function as plotted in Fig. 3a in the main text.

Medaka aging and population dynamics in ponds

Medaka juveniles are too small to be tagged and, unlike in Japan (Terao 1985; Edeline *et al.* 2016), no winter check was deposited in medaka otoliths in our experimental populations. We therefore relied on an analysis of body length-frequency distributions to infer medaka age using model-based clustering in the `mclust` R package (Scrucca *et al.* 2016). Medaka longevity ranges from one year in the wild in Japan to five years in the laboratory (Edeline et al. 2016 and references therein). Therefore, we allowed for one to five Gaussian component models and further allowed for different variances between the Gaussian components. Then, we selected the optimal model and corresponding number of Gaussian components according to Bayesian Information Criterion, as returned by the `mclustBIC` function (the optimal model was that yielding the highest BIC value).

We estimated medaka population dynamics in ponds through their stock-recruitment relationship, where stock in the total number of fish in March (i.e., number of age 0+ and 1+ individuals) and recruitment is the number of age 0+ individuals in Autumn of the same year. To estimate recruitment, we fitted a mixture of two Gaussian distributions to individual standard body lengths Sdl:

$$\begin{aligned} & Sdl_i \sim \sum_{j=1}^{J} \sum_{k=1}^{K} \pi_{j,k} N\left(\mu_{j,k}, \sigma_j^2\right) \\ & \mu_{2,k} \sim N\left(\mu_{H[k]}, \sigma^2\right) \\ & \mu_{1,k} = \delta_k \mu_{2,k} \\ & \delta_k \sim U(0,1) \end{aligned} \qquad \text{(1a),}$$

where i indexes individuals (n = 17908), j indexes age groups (age 0+ *vs*. 1+ such that $J = 2$), k indexes a sampling event, i.e., indexes one population in a particular year and month ($K = 109$ sampling events), N is the normal distribution, and U is the uniform distribution. $H[k]$ indexes the harvest treatment (harvested *vs*. non harvested) associated with sampling event k . $\pi_{j,k}$ is the proportion of age j individuals at each sampling event k such as for each k :

$$\pi_j \geq 0, \sum_{j=1}^{J} \pi_j = 1 \qquad \text{(1b).}$$

Indexes in line 1 in Eq. 1a show that our model estimated a mean standard body length separately for each age group at each sampling event, while body length variance was assumed to vary only with age. Line 2 in Eq. 1a shows that we assumed the mean standard body length at age 1+ at each sampling event, $\mu_{2,k}$, to be a normally-distributed random variable with higher-hierarchical mean specific to each harvest treatment, because harvesting was expected to restrict the maximum body size of medaka. Lines 3-4 in Eq. 1a show that mean standard body length of age 0+ medaka at each sampling event, $\mu_{1,k}$, was estimated as proportional to $\mu_{2,k}$ with a proportionality constant δ_k following a uniform distribution between 0 and 1. Model 1 provided us with MCMC (see below) age samples for each individual fish in the dataset, allowing us to compute age-specific exploitation rates by the fishery that were on average 58% (95% credible interval 34-72 %) on age 0+ juveniles, and 96 % (95% credible interval 92-98 %) on age 1+ adults.

Model (1) above allowed us to estimate the absolute number R_k of age 0+ medaka recruits at each November sampling event k (*n* = 60 November sampling events). We then visualized the strength of negative density-dependence in pond medaka populations by plotting (Fig. 3b in the main text) Ricker “stock-recruitment” relationships between R_k and the number S_k of fish released in March (stock of spawners):

$$\begin{aligned} &R_k \sim P(\lambda_k) \\ &\ln(\lambda_k) = \ln(S_k) + \alpha_{Year[k]} + \beta_{Year[k]} S_k \end{aligned} \quad (3),$$

where P is the Poisson distribution and $Year[k]$ indexes indicate that one Ricker curve was fitted for each year from 2012 to 2016.

Larvae counts

Larvae counts L were highly overdispersed and followed a zero-inflated negative binomial distribution, which we modelled as (Ntzoufras 2009):

$$\begin{aligned} &L_i \sim NB(\phi_i, r_{H[i]}) \\ &\phi_i = \frac{r_{H[i]}}{r_{H[i]} + \lambda_i (1 - \theta_i)} \\ &\ln(\lambda_i) = \alpha_{k[i]} + \beta_{H[i]} + \gamma_{H[i]} Day_i + \delta_{H[i]} Day_i^2 \\ &\alpha_{k[i]} \sim N(0, \sigma_\alpha^2) \end{aligned} \quad (4a),$$

where NB is the negative binomial distribution with success probability ϕ and number of failures r, and subscript i indexes counts from a given observer in a given population on a given sampling day (*n* = 2004 counts). Lines 3 and 4 in Eq. (4a) show that we modelled positive (non-zero) counts λ

as a harvest treatment-specific, 2nd order polynomial of the day of year (scaled to 0 mean), with a normally-distributed random effect of k corresponding, as above, to a given population in a given year (n = 36).

The θ latent variable for absence of larvae was modelled as a Bernoulli process being a 2nd order polynomial of the day of year :

$$\begin{aligned} &\theta_i \sim B(\psi_i) \\ &\ln\left(\frac{\psi_i}{1-\psi_i}\right) = \epsilon + \zeta\, Day_i + \eta\, Day_i^2 \end{aligned} \quad \text{(4b),}$$

where B is the Bernoulli distribution with probability of larvae absence ψ .

Line 2 in Eq. 4a shows that we allowed for the r parameter, which enters in the computation of the variance of the distribution (Ntzoufras 2009), to be different among the two harvest treatments H . Harvest treatment-specific mean larvae count is given by $E(L_H) = \bar{\lambda}_H (1-\bar{\theta})$ and variance by $var(L_H) = \bar{\lambda}_H (1-\bar{\theta})(\bar{\lambda}_H (1-\bar{\theta}) + r_H)$. In Table S1, we computed the dispersion index in each harvest treatment as $DI_H = E(L_H) / var(L_H)$ (Ntzoufras 2009).

Zooplankton and filamentous algae in ponds

We estimated the effect of medaka fishing on zooplankton abundances (*n* = 960 observations) using a zero-inflated negative binomial GLMM (e.g., model 4 described above). The linear predictor was the same for both positive counts and the latent variable for absence, and included as fixed effects a medaka fishing-by-zooplankton taxon interaction (*n* = 2*6 = 12 levels), and as normally-distributed random intercepts the pond (*n* = 12 levels), sampling date (*n* = 11 levels), and enumeration method (*n* = 3 levels). We estimated an effect of medaka fishing on % of pond covered by filamentous algae (*n* =

234 observations) using a negative binomial GLMM that included as fixed effect medaka fishing (n = 2 levels) and as random intercepts the pond (n = 12 levels), sampling date (n = 7 levels) and the observer (n = 9 levels).

Somatic growth rates and trajectories of F_1 progeny in the laboratory

We estimated harvest-by-food interactions on medaka growth trajectories using a 2nd order polynomial regression of standard body length Sdl on age (measured in days-post-hatch):

$$\begin{aligned}
&Sdl_i \sim N(\mu_i, \sigma_i^2)\\
&\mu_i = \alpha_{P[i]} + \beta_{H[i]} + (\gamma_{H[i],F[i]} + \delta_{P[i]}) * Age_i + \eta\, Age_i^2\\
&\alpha_{P[i]} \sim N(0, \sigma_\alpha^2)\\
&\delta_{P[i]} \sim N(0, \sigma_\delta^2)\\
&\ln(\sigma_i^2) = \mathrm{A}_{H[i],F[i]} + \mathrm{B}_{H[i],F[i]}\, Age_i
\end{aligned} \qquad (5),$$

where i indexes length observations (n = 1144 observations from 104 individuals), $H[i]$ indexes the harvest treatment associated with observation i (n = 2 levels), $H[i], F[i]$ indexes the interaction of harvest treatment and food environment (n = 2 * 3 = 6 levels), and $P[i]$ indexes the parental breeding pair associated with observation i (n = 36 pairs), treated as a normally-distributed random effect on both size-at-hatch α and the linear somatic growth rate γ . The six γ parameters in Eq. 5 estimate the slope of the age effect on Sdl and provided somatic growth rates as plotted in Fig. 5a of the main text. The random pair effects on somatic growth rate, δ_P , are shown in Fig. S2.

In this model, we assumed both linear somatic growth rate γ and the regression of (ln-transformed) residuals variance on age to be different among harvest treatments and food environments (lines 2 and

5 in Eq. 5, respectively). In contrast, size-at-hatch $\beta_{H[i]}$ was allowed to vary only due to harvest treatment because food environments were applied only starting from 15 dph.

Probabilistic maturation reaction norms of F_1 progeny in the laboratory

Probabilistic maturation reaction norms (PMRNs) describe the probability that an immature individual at a given age and size will mature during a given interval of time (Heino *et al.* 2002). Provided that plasticity in the maturation process is captured by growth trajectories, PMRNs separate the effects of evolution from plasticity on maturation. PMRNs have been extensively used to explore genetic effects of exploitation on the maturation process in wild populations (Olsen *et al.* 2004; Heino & Dieckmann 2008). We fitted a Bernouilli model to individual medaka maturity (0 or 1) data y_i, truncated so as to keep only the first maturity event for each individual (Heino & Dieckmann 2008):

$$\begin{aligned} & y_i \sim B(\mathrm{M}_i) \\ & \ln\left(\frac{\mathrm{M}_i}{1-\mathrm{M}_i}\right) = \alpha_{P[i]} + \beta_{H[i]} + \gamma_{H[i]} Age_i + \delta_{H[i]} Sdl_i \\ & \alpha_{P[i]} \sim N(0, \sigma_\alpha^2) \end{aligned} \qquad (6),$$

where M is maturity probability. Other subscripts or variables are as described in Eq. 5. The random pair effects on maturation probability at an average age and length, α_P, shown in Fig. S2.

Maturation rates of F_1 progeny in the laboratory

Technically, the PMRN approach assumes that observations are made at regular time intervals and, biologically, PMRNs assume that maturation is a discrete event. In the reality, however, observations are often made at irregular intervals (e.g., we observed medaka at intervals ranging from 6 to 17 days, 10 days on average), and maturation is often the threshold phenotypic expression of a continuous physiological process (Harney et al. 2013 and references therein). To bypass these problems, maturation rate models were developed that are not sensitive to the periodicity of observations and can more finely capture the physiological dynamics that underlie maturation (Van Dooren *et al.* 2005). Harney et al. (2013) have shown that maturation rate models may be approximated by fitting maturation data to standard GLMs:

$$\begin{aligned} & y_i \sim B(\mathrm{M}_i) \\ & \ln\left(\frac{\mathrm{M}_i}{1-\mathrm{M}_i}\right) = \ln(\Delta_i) + \alpha_{P[i]} + \beta_{H[i],F[i]} + \gamma\, Age_i + \delta\, Sdl_i \\ & \alpha_{P[i]} \sim N(0, \sigma_\alpha^2) \end{aligned} \qquad (7),$$

where subscripts are similar to that described in Eq. 6, and the duration interval (days) between two observations Δ is included as an offset term. We used this approach to estimate harvest-by-food interaction on medaka maturation rates, in complement with the PMRN approach described above. The parameter β captures maturation rates (in logit of maturation probability day^{-1}), as plotted in Fig. 5b in the main text.

Predatory behaviour of F$_1$ progeny in the laboratory

Counts C_i of number of prey eaten by individual medaka followed a zero-inflated negative binomial distribution and were modelled similarly to larvae counts in model 4 above:

$$\begin{aligned} & C_i \sim NB(\phi_i, r_{H[i],F[i]}) \\ & \phi_i = \frac{r_{H[i],F[i]}}{r_{H[i],F[i]} + \lambda_i (1-\theta_i)} \\ & \ln(\lambda_i) = \alpha_{I[i]} + \beta_{H[i],F[i]} \\ & \alpha_{I[i]} \sim N(0, \sigma_\alpha^2) \end{aligned} \qquad (8a),$$

where number of failures r and positive (non-zero) counts λ were both modelled as being different among harvest treatments H in each food environment F, while $\alpha_{I[i]}$ was a normally-distributed random individual effect on λ (n = 104 individuals). The θ latent variable was modelled as:

$$\begin{gathered}\theta_i \sim B(\psi_i)\\ \ln\left(\frac{\psi_i}{1-\psi_i}\right)=\gamma+\delta_{I[i]} \quad \text{(8b),}\\ \delta_{I[i]} \sim N(0,\sigma_\delta^2)\end{gathered}$$

where δ_I is a normally-distributed random individual effect.

Analysis of deviance

We tested for the overall statistical significance of harvest-by-food interactions on somatic growth and maturation in the laboratory using analyses of deviance. Specifically, we fitted the following models:

$$\begin{gathered}Sdl_i \sim N(\mu_i,\sigma^2)\\ \mu_i=\alpha_{H[i]}+\left(\beta_{H[i]}+\gamma_{F[i]}+\delta_{H[i],F[i]}\right)Age_i+\epsilon\, Age_i^2\end{gathered} \qquad \text{(9), and}$$

$$\begin{gathered}y_i \sim B(\mathrm{M}_i)\\ \ln\left(\frac{\mathrm{M}_i}{1-\mathrm{M}_i}\right)=\alpha_{H[i]}+\beta_{F[i]}+\gamma_{H[i],F[i]}+\left(\delta_{H[i]}+\epsilon_{F[i]}+\zeta_{H[i],F[i]}\right)Age_i+\left(\eta_{H[i]}+\theta_{F[i]}+\iota_{H[i],F[i]}\right)Sdl_i\end{gathered} \qquad \text{(10),}$$

where variables and indexes are as in models (5) and (6).

Parameter estimation

Models 3, 9 and 10 were fitted using maximum likelihood (`glm` function, “`quasibinomial`” distribution for Eq. 10) in R 3.6.1 (R Core Team 2019). Analysis of deviance for models 9 and 10 was performed with the `anova` function using an F test to evaluate the significance of each predictor separately (Table S3). Models for the abundance of zooplankton and for % of pond covered by filamentous algae were fitted by maximum likelihood using the `glmmTMB` library of the R software (Brooks *et al.* 2017). Other models were fitted by Markov chain Monte Carlo (MCMC) in JAGS 4.2.0 (Plummer 2003) through the jagsUI package (Kellner 2019). To ease model convergence and avoid slope-intercept correlations, all numerical predictors were scaled to zero mean and, in case of Bernoulli distributions with logit links, further standardized to 0.5 standard deviation (Gelman *et al.* 2008). For each model, we ran three independent MCMC chains thinned at a period of 5 iterations until parameter convergence was reached, as assessed using the Gelman–Rubin statistic (Gelman & Rubin 1992).

Parameter estimates for models 4-6 and 8 are provided in Table S2. Statistical significance of harvest- and food-treatment effects reported in the main text was assessed from the posterior distributions of parameter differences in a test equivalent to a bilateral *t* test. In these tests, the MCMC P-value was twice the proportion of the posterior for which the sign was opposite to that of the mean posterior value. Priors were chosen to be weakly informative. In model 1 we used a Dirichlet prior for $\pi_{j,k}$ and prevented label switching by assigning age class 0+ to fish shorter than 8 mm and age class 1+ and older to fish longer than 35 mm (Chung *et al.* 2004).

We assessed goodness of fit of our models by using a Bayesian P-value (Gelman *et al.* 1996). Briefly, we computed residuals for the actual data as well as for synthetic data simulated from estimated model parameters (i.e., residuals from fitting the model to ‘‘ideal’’ data). The Bayesian P-value is the proportion of simulations in which ideal residuals are larger than true residuals. If the model fits the data well, the Bayesian P-value is close to 0.5. Bayesian P values for our models ranged from 0.47 to 0.57 and were on average 0.51, indicating excellent model fit to the data.

APPENDIX II. NATURAL SELECTION ON BODY SIZE IN MEDAKA

We suggest that natural selection favoured small-bodied medaka in the wild, but large-bodied medaka in ponds. In the wild, medaka starve to death during their first reproductive bout while reaching age 1+, suggesting that small-bodied juvenile medaka exclude their large-bodied parents in exploitative competition for food (Edeline et al. 2016 and references therein). This is presumably because the complex habitat structure and relatively low population densities that prevail in the wild reduce interference and make competition to operate mainly through food exploitation, in which case a small body size provides fish with a strong competitive advantage (Persson *et al.* 1998; Persson & De Roos 2006). This natural selection regime in the wild was shifted in our experimental ponds, where overcompensating stock-recruitment curves mediated by increased juvenile mortality demonstrate that large-bodied adults dominated small-bodied juveniles. Compared to the wild, ponds had drastically reduced habitat complexity and probably also higher population densities. These environmental changes likely shifted competition to operate mainly through interference, which was shown to favour larger body sizes in multiple systems (Post *et al.* 1999; Calsbeek & Smith 2007; Reichstein *et al.* 2013; Le Bourlot *et al.* 2014). In fish, interference is often associated with cannibalism which also favours larger body sizes (Claessen *et al.* 2000, 2004).

APPENDIX III: SUPPLEMENTARY RESULTS

Table. S1. Inference of number of age classes in pond medaka populations from body length distributions using model-based clustering. Models including one to five Gaussian components were fitted to body-lengths separately for each year and harvest treatment. The optimal number of Gaussian components was that corresponding to the model returning the highest BIC (Scrucca *et al.* 2016).

Harvest treatment	Year	Optimal number of Gaussian components
Harvested	2012	2
	2013	2
	2014	2
	2015	1
	2016	2
Unharvested	2012	2
	2013	2
	2014	2
	2015	2
	2016	2

Table S2. Structure and MCMC parameter estimates for models 4-6 and 8. The MCMC P-value is twice the proportion of the posterior for which the sign was opposite to that of the mean posterior value. MCMC P-values are not relevant for variance parameters that are constrained to be non-zero.

Response	N	Distribution	Link	Effect	Mean estimate	SD of the estimate	MCMC P-value
Larvae count	2004	Bernoulli in ZINB	logit	Int.	-8.254	1.385	0.000
				Slope of day	-6.703	1.008	0.000
				Slope of day squared	10.356	1.800	0.000
		Negative binomial in ZINB	ln	Int. no-harvest	2.167	0.250	0.000
				Int. harvest	1.250	0.251	0.000
				Slope of day no-harvest	0.292	0.080	0.000
				Slope of day harvest	2.211	0.141	0.000
				Slope of day squared no-harvest	-0.472	0.127	0.000
				Slope of day squared harvest	-1.638	0.182	0.000
				Dispersion index no-harvest	5.372	1.125	
				Dispersion index harvest	3.996	0.780	
				SD of year by pond effect (random)	0.977	0.133	
Standard body length	1144	Gaussian	Identity	Int. no-harvest	4.410	0.106	0.000
				Int. harvest	4.548	0.099	0.000
				Slope of age no-harvest low food	0.224	0.005	0.000
				Slope of age harvest low food	0.210	0.005	0.000
				Slope of age no-harvest medium food	0.250	0.005	0.000
				Slope of age harvest medium food	0.231	0.005	0.000
				Slope of age no-harvest high food	0.263	0.005	0.000
				Slope of age harvest high food	0.248	0.004	0.000
				Slope of age squared	-0.001	0.000	0.000
				Int. residual variance no-harvest low food	-0.012	0.149	0.921
				Int. residual variance harvest low food	-0.547	0.123	0.000
				Int. residual variance no-harvest medium food	-0.605	0.149	0.000
				Int. residual variance harvest medium food	-0.377	0.138	0.007
				Int. residual variance no-harvest high food	-0.534	0.130	0.001
				Int. residual variance harvest high food	-0.296	0.151	0.063
				Slope of age residual variance no-harvest low food	-0.005	0.003	0.063
				Slope of age residual variance harvest low food	0.011	0.002	0.000
				Slope of age residual variance no-harvest medium food	0.000	0.003	0.985
				Slope of age residual variance harvest medium food	0.010	0.002	0.000
				Slope of age residual variance no-harvest high food	0.011	0.002	0.000
				Slope of age residual variance harvest high food	-0.011	0.003	0.001
				SD of parental pair effect on int. (random)	0.014	0.002	
				SD of parental pair on slope of Age effect (random)	0.303	0.069	

Continues on the next page.

Table S2 continued.

Response	N	Distribution	Link	Effect	Mean estimate	SD of the estimate	MCMC P-value
Maturation probability	591	Bernoulli	logit	Int. no-harvest low food	-8.372	0.922	0.000
				Int. harvest low food	-6.477	0.723	0.000
				Int. no-harvest medium food	-6.009	0.685	0.000
				Int. harvest medium food	-5.905	0.626	0.000
				Int. no-harvest high food	-6.063	0.735	0.000
				Int. harvest high food	-6.544	0.676	0.000
				Slope of age	1.554	0.908	0.090
				Slope of length	7.247	1.164	0.000
				SD of parental pair effect on int. (random)	1.469	0.355	
Prey count	311	Bernoulli in ZINB	logit	Int.	-1.960	0.541	0.000
				SD of individual effect (random)	0.903	0.534	
		Negative binomial in ZINB	ln	Int. no-harvest, low food	2.035	0.208	0.000
				Int. harvest, low food	1.848	0.231	0.000
				Int. no-harvest, medium food	1.928	0.245	0.000
				Int. harvest, medium food	0.986	0.286	0.001
				Int. no-harvest, high food	0.357	0.270	0.188
				Int. harvest, high food	0.672	0.309	0.025
				Dispersion index no-harvest, low food	2.388	0.722	
				Dispersion index harvest, low food	5.994	2.141	
				Dispersion index no-harvest, medium food	6.509	3.857	
				Dispersion index harvest, medium food	5.012	2.357	
				Dispersion index no-harvest, high food	2.033	0.710	
				Dispersion index harvest, high food	5.708	2.642	
				SD of individual effect (random)	0.681	0.136	

Table S3. Effect of medaka fishing on medaka food in ponds. Zooplankton abundances are counts per liter and abundances of filamentous algae are % of pond surface covered. Predictions were obtained from statistical models described in the SI Appendix I. There was a large variability in zooplankton counts due to the effects of the pond, sampling date and enumeration method, and the positive effect of medaka fishing was statistically significant on *Asplanchna* sp. (probability of presence, $p = 0.033$), copepodites of calanoids (non-zero abundances, $p < 0.001$) and Cladocerans (non-zero abundances, $p < 0.001$) before June but not after (results not shown), probably because of medaka recruitment that increased medaka density in unharvested ponds. The effect of medaka fishing on filamentous algae was statistically significant ($p < 0.002$).

Taxa	**Medaka treatment**	**Predicted Count / L (zooplankton) or % pond surface cover (filamentous algae)**	
		Mean	**SE**
Asplanchna sp.	Harvested	14.2	15.5
	Unharvested	8.5	9.6
Copepodites of calanoids	Harvested	161.6	150.0
	Unharvested	85.2	79.1
Cladocerans	Harvested	51.4	48.1
	Unharvested	18.1	17.1
Copepodites of cyclopoids	Harvested	2.7	2.6
	Unharvested	3.2	3.1
Copepod *nauplii*	Harvested	213.3	197.6
	Unharvested	215.2	199.8
Small rotifers	Harvested	7018.9	6537.0
	Unharvested	6939.2	6458.5
Filamentous algae	Harvested	18.5	11.5
	Unharvested	1.3	0.8

Table S4. Analysis of deviance for GLMs testing for the harvest-by-food interaction on life-history traits in laboratory-born F_1 medaka progeny. The "Deviance" column gives the reduction in the residual deviance as each predictor is added in turn into the model. The P-values compare the reduction in deviance to the residual deviance in an F test.

Trait	Distribution	Link	Predictor	Df	Deviance	Resid. DF	Resid. Dev	F	P-val
Body length	Gaussian	Identity	Harvesting	1	163	1130	20588	155	**<0.0001**
			Food	2	658	1128	19929	312	**<0.0001**
			Age	1	18086	1127	1843	17124	**<0.0001**
			Age^2	1	469	1126	1374	444	**<0.0001**
			Harvesting x Food	2	2	1124	1372	1	0.3282
			Harvesting x Age	1	22	1123	1350	21	**<0.0001**
			Food x Age	2	167	1121	1183	79	**<0.0001**
			Harvesting x Food x Age	2	1	1119	1182	0	0.7160
Maturation	Bernoulli	Logit	Harvesting	1	0	589	528	0	0.5758
			Food	2	6	587	522	6	**0.0041**
			Age	1	135	586	387	253	**<0.0001**
			Length	1	57	585	329	107	**<0.0001**
			Harvesting x Food	2	7	583	323	6	**0.0022**
			Harvesting x Age	1	3	582	320	5	**0.0195**
			Food x Age	2	11	580	309	11	**<0.0001**
			Harvesting x Length	1	0	579	308	0	0.5630
			Food x Length	2	2	577	307	2	0.2142
			Harvesting x Food x Age	2	15	575	292	14	**<0.0001**
			Harvesting x Food x Length	2	1	573	290	1	0.3197

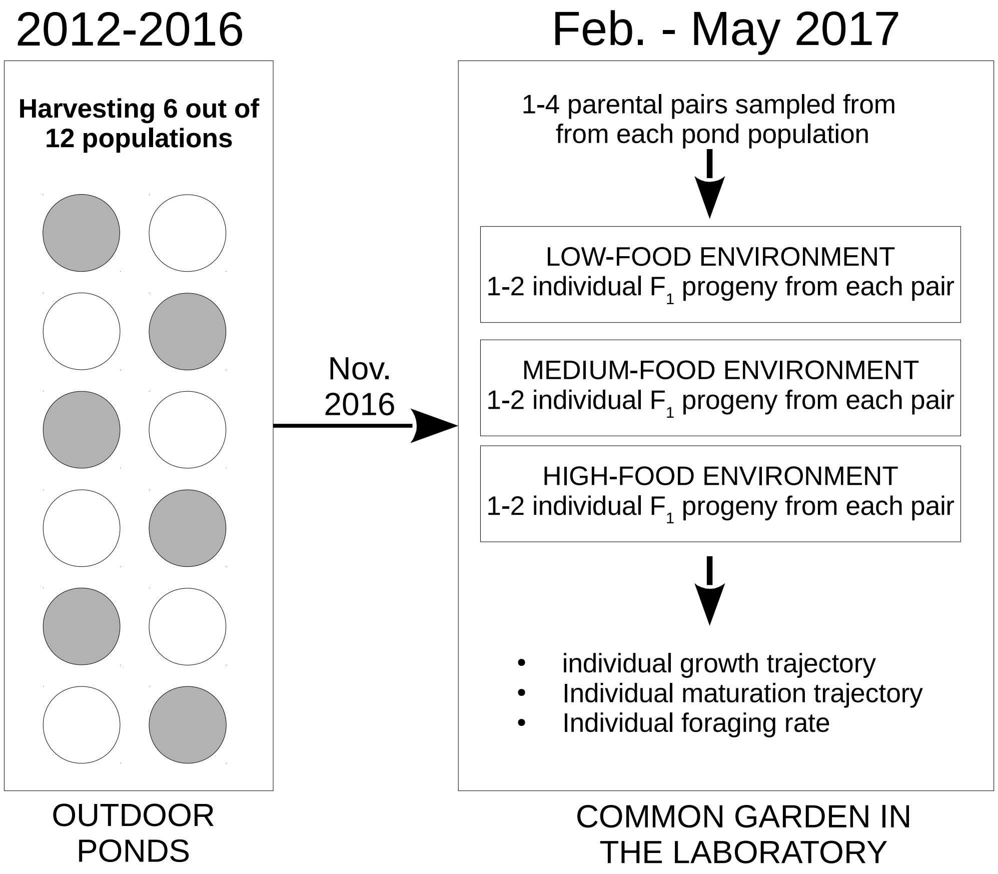

Fig. S1. Experimental design. In 2012, 12 independent populations of medaka were introduced in 12, 10 m^2 outdoor ponds and maintained naturally with no added food. Each year from 2012 to 2016, the 12 populations were sampled (98% catch rate) in March and November, and each fish was individually weighed. Each year in March in six populations (shaded), only the 19% smallest-bodied individuals from the catch were released, while all individuals were released in the other six populations (unshaded). Each year in November, all fish were released after weighing, except in November 2016 when a random sample of 6-10 fish (mean 9.6) from each population was kept and transferred to the laboratory to serve as parents in a common garden experiment. In 2017, parents originating from the same population were mated and their progeny was distributed in individual tanks under three food environments (Low, Medium, High), where we measured their individual somatic growth rate, maturation trajectory, and foraging rate.

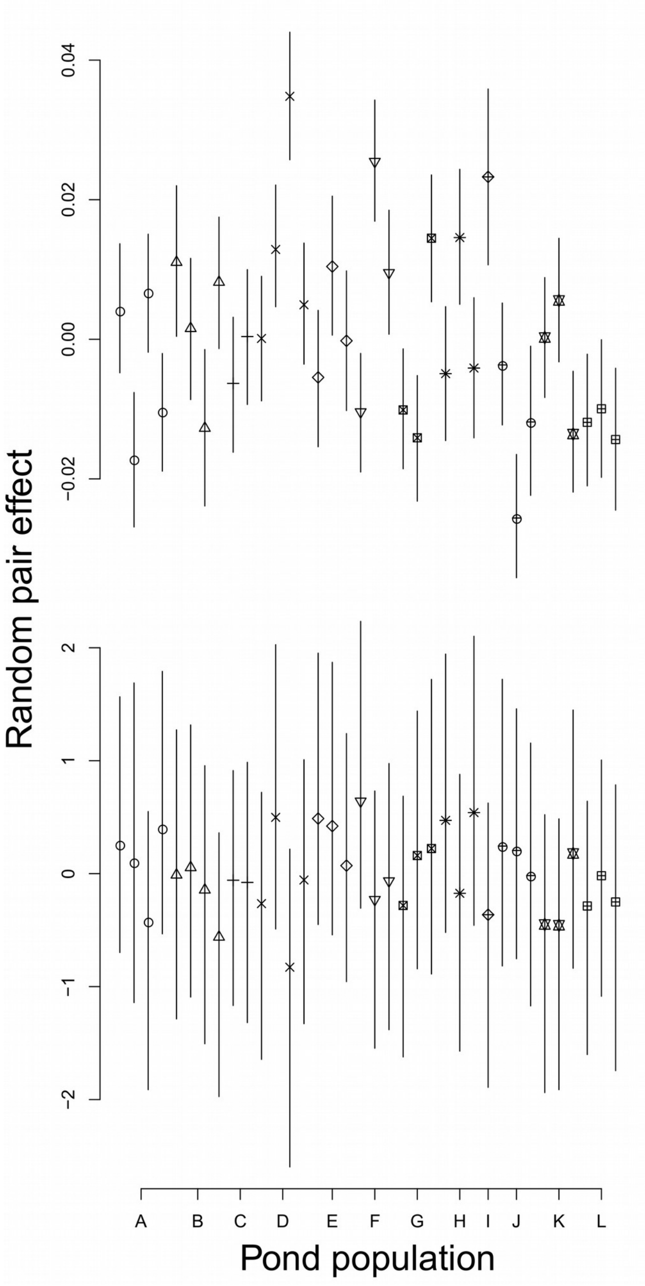

Fig. S2. Random effects of breeding pairs on the somatic growth rate (top) and maturation probability (bottom) of F_1 medaka progeny in the laboratory. Effects were estimated by MCMC from models 5 and 6, as described above. Points show median MCMC estimates with 95% credible intervals. Effects for somatic growth rate are in mm day^{-1} and effects on maturation are in logit (probability). Symbols correspond to the pond population of origin (coded on the x axis from A to L). Populations A, D, F, G, J and K were harvested while other populations were unharvested.

368

Supplementary References

Brooks, M.E., Kristensen, K., Benthem, K.J. van, Magnusson, A., Berg, C.W., Nielsen, A., *et al.* (2017). glmmTMB balances speed and flexibility among packages for zero-inflated generalized linear mixed modeling. *R J.*, 9, 378–400.

Brown, J.H., Gillooly, J.F., Allen, A.P., Savage, V.M. & West, G.B. (2004). Toward a metabolic theory of ecology. *Ecology*, 85, 1771–1789.

Calsbeek, R. & Smith, T.B. (2007). Probing the adaptive landscape using experimental islands: density-dependent natural selection on lizard body size. *Evol. Int. J. Org. Evol.*, 61, 1052–1061.

Chung, H., Loken, E. & Schafer, J.L. (2004). Difficulties in drawing inferences with finite-mixture models: a simple example with a simple solution. *Am. Stat.*, 58, 152–158.

Claessen, D., de Roos, A.M. & Persson, L. (2000). Dwarfs and giants: cannibalism and competition in size structured populations. *Am. Nat.*, 155, 219–237.

Claessen, D., de Roos, A.M. & Persson, L. (2004). Population dynamic theory of size-dependent cannibalism. *Proc. R. Soc. Lond. B Biol. Sci.*, 271, 333.

Edeline, E., Terao, O. & Naruse, K. (2016). Empirical evidence for competition-driven semelparity in wild medaka. *Popul. Ecol.*, 58, 371–383.

Gelman, A., Jakulin, A., Pittau, M.G. & Su, Y.-S. (2008). A weakly informative default prior distribution for logistic and other regression models. *Ann. Appl. Stat.*, 2, 1360–1383.

Gelman, A., Meng, X.L. & Stern, H. (1996). Posterior predictive assessment of model fitness via realized discrepancies. *Stat. Sin.*, 6, 733–807.

Gelman, A. & Rubin, D.B. (1992). Inference from iterative simulation using multiple sequences. *Stat. Sci*, 457–472.

Gorsky, G., Ohman, M.D., Picheral, M., Gasparini, S., Stemmann, L., Romagnan, J.-B., *et al.* (2010). Digital zooplankton image analysis using the ZooScan integrated system. *J. Plankton Res.*, 32, 285–303.

Harney, E., Van Dooren, T.J.M., Paterson, S. & Plaistow, S.J. (2013). How to measure maturation: a comparison of probabilistic methods used to test for genotypic variation and plasticity in the decision to mature. *Evolution*, 67, 525–538.

Heino, M. & Dieckmann, U. (2008). Detecting fisheries-induced life-history evolution: an overview of the reaction-norm approach. *Bull. Mar. Sci.*, 83, 69–93.

Heino, M., Dieckmann, U. & Godø, O.R. (2002). Measuring probabilistic reaction norms for age and size at maturation. *Evolution*, 56, 669–678.

Kellner, K. (2019). *jagsUI: a wrapper around "rjags" to streamline "JAGS" analyses*.

Le Bourlot, V., Tully, T. & Claessen, D. (2014). Interference versus exploitative competition in the regulation of size-structured populations. *Am. Nat.*, 184, 609–623.

Ntzoufras, I. (2009). *Bayesian modeling using WinBUGS*. 1st edn. Wiley, Hoboken (NJ).

Olsen, E.M., Heino, M., Lilly, G.R., Morgan, M.J., Brattey, J., Ernande, B., *et al.* (2004). Maturation trends indicative of rapid evolution preceded the collapse of northern cod. *Nature*, 428, 932–935.

Persson, L. & De Roos, A.M. (2006). Food-dependent individual growth and population dynamics in fishes. *J. Fish Biol.*, 69, 1–20.

Persson, L., Leonardsson, K., de Roos, A.M., Gyllenberg, M. & Christensen, B. (1998). Ontogenetic scaling of foraging rates and the dynamics of a size-structured consumer-resource model. *Theor. Popul. Biol.*, 54, 270–293.

Plummer, M. (2003). JAGS: a program for analysis of Bayesian graphical models using Gibbs sampling. Presented at the Proceedings of the 3rd international workshop on distributed statistical computing, Vienna, Austria.

Post, J.R., Parkinson, E.A. & Johnston, N.T. (1999). Density-dependent processes in structured fish populations: interaction strengths in whole-lake experiments. *Ecol. Monogr.*, 69, 155–175.

R Core Team. (2019). *R: a language and environment for statistical computing*. R Foundation for Statistical Computing, Vienna, Austria.

Reichstein, B., Schröder, A., Persson, L. & De Roos, A.M. (2013). Habitat complexity does not promote coexistence in a size-structured intraguild predation system. *J. Anim. Ecol.*, 82, 55–63.

Renneville, C., Millot, A., Agostini, S., Carmignac, D., Maugars, G., Dufour, S., *et al.* (in press). Unidirectional response to bidirectional selection on body size. I. Phenotypic, life history and endocrine response. *Ecol. Evol.*

Scrucca, L., Fop, M., Murphy, T.B. & Raftery, A.E. (2016). mclust 5: clustering, classification and density estimation using Gaussian finite mixture models. *R J.*, 8, 289–317.

Sieracki, C.K., Sieracki, M.E. & Yentsch, C.S. (1998). An imaging-in-flow system for automated analysis of marine microplankton. *Mar. Ecol. Prog. Ser.*, 168, 285–296.

Terao, O. (1985). Contribution to the study of the ecology of the medaka, *Oryzias latipes,* under natural conditions: life span, reproduction, food habits and its seasonal changes. Master Thesis. Tokyo.

Van Dooren, T.J.M., Tully, T. & Ferrière, R. (2005). The analysis of reaction norms for age and size at maturity using maturation rate models. *Evolution*, 59, 500–506.